



Short Communication

The FDA-approved drugs ticlopidine, sertaconazole, and dexlansoprazole can cause morphological changes in *C. elegans*

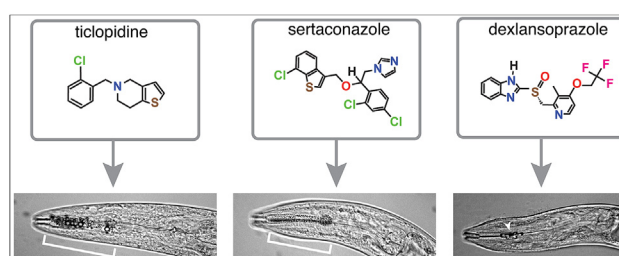
Kyle F. Galford, Antony M. Jose*

Department of Cell Biology and Molecular Genetics, University of Maryland, College Park, MD, 20742, USA

HIGHLIGHTS

- The nematode *C. elegans* was modified to make a drug-sensitive strain.
- Three FDA-approved drugs found using the strain can alter wild-type *C. elegans*.
- Ticlopidine and Sertaconazole cause accumulations & lethality upon acute exposure.
- Dexlansoprazole causes defects in molting upon exposure during larval development.

GRAPHICAL ABSTRACT



ARTICLE INFO

Article history:

Received 5 May 2020

Received in revised form

13 July 2020

Accepted 14 July 2020

Available online 23 July 2020

Handling Editor: Willie Peijnenburg

Keywords:

Molting

Marginal cells

Epigenetic sensor

Toxicology

Genetic screen

ABSTRACT

Urgent need for treatments limit studies of therapeutic drugs before approval by regulatory agencies. Analyses of drugs after approval can therefore improve our understanding of their mechanism of action and enable better therapies. We screened a library of 1443 Food and Drug Administration (FDA)-approved drugs using a simple assay in the nematode *C. elegans* and found three compounds that caused morphological changes. While the anticoagulant ticlopidine and the antifungal sertaconazole caused both accumulations that resulted in distinct distortions of pharyngeal anatomy and lethality upon acute exposure, the proton-pump inhibitor dexlansoprazole caused molting defects and required exposure during larval development. Such easily detectable defects in a powerful genetic model system advocate the continued exploration of current medicines using a variety of model organisms to better understand drugs already prescribed to millions of patients.

© 2020 The Author(s). Published by Elsevier Ltd. This is an open access article under the CC BY-NC-ND license (<http://creativecommons.org/licenses/by-nc-nd/4.0/>).

1. Introduction

Imperfect knowledge about biology makes it difficult to anticipate all the effects of a drug and makes empirical testing necessary. The extent of testing needed, however, is often unclear. Famously, the sedative thalidomide taken by pregnant women for morning

sickness caused birth defects in more than 10,000 babies (McBride, 1961; Lenz et al., 1962) possibly through the degradation of a transcription factor required for limb development (Donovan et al., 2018; Matyskiela et al., 2018) - a mechanism that has taken more than 50 years to elucidate. Ideally, a drug would be tested for efficacy and side effects under many circumstances during the lifetime of individuals and even their descendants. Such comprehensive testing, however, is impractical because of pressing needs for medicines to alleviate suffering. Adequate risk assessment of a drug before approval can also be stymied by latency or underreporting of adverse side effects. For example, the cardiovascular risks of using

* Corresponding author. Rm 2136, Bioscience Research Building (Bldg #413), University of Maryland, College Park, MD, 20742, USA.

E-mail address: amjose@umd.edu (A.M. Jose).

the COX-2-selective nonsteroidal anti-inflammatory drug rofecoxib was only established more than five years after its approval (Krumholz et al., 2007). Aware of such risks with every approved drug, regulatory agencies continue to monitor unanticipated effects after approval (e.g. the Food and Drug Administration (FDA) (MedWatch, 2020)). This wait-and-watch strategy could be complemented with proactive analyses of the effects of approved drugs in a variety of model systems. With the approval of 59 new drugs by the FDA in 2018 (Mullard, 2019) the need for such post-approval studies has heightened.

Most drug testing is done using mice and other mammals under the premise that they have more human-like features. However, such complex animal models can be difficult to work with and are less characterized than simpler animal models that nevertheless capture some fundamental molecular features of human biology. For example, the nematode *C. elegans* has 7943 genes with human orthologs (Kim et al., 2018) and uses many conserved mechanisms, including signaling through G-protein coupled receptors that are similar to those most frequently targeted by drugs in humans (Overington et al., 2006). In recognition of these features, *C. elegans* has been proposed as a potentially effective model for detecting toxicity of new compounds (Ferreira et al., 2014; Hunt, 2017). Such expansion of the set of model systems to test adverse effects of compounds is also supported by the prior inability of popular mammalian models to reveal human toxicity (for example, the harmful effects of thalidomide are detected in rabbits but not in mice (Fratta et al., 1965)). Complementing such toxicity studies with deep analyses on the effects of compounds that have been approved for treating human diseases could be similarly productive. The extensive characterization of *C. elegans* (Kaletta and Hengartner, 2006) and its short generation time make it ideally suited for testing the effects of a drug under many circumstances throughout the lifetime of individuals and their descendants.

The first step to discover if a model system could be useful for the analysis of a drug, is to determine if there is any measurable change induced by the drug. These changes could range from obvious effects that are detectable using simple assays to subtle effects that require sophisticated molecular measurements. Any such interactions would only be the starting point for subsequent mechanistic analyses, which could either reveal information of immediate relevance to human health or provide insights into the properties of the drug that could help future development. Here we report our serendipitous discovery of obvious morphological changes in the nematode *C. elegans* caused by drugs in current use.

2. Materials and methods

2.1. *C. elegans* culture

Worm strains (N2: wild type, EG6787: *oxSi487 [Pmex-5::mCherry::h2b::tbb-2 3'UTR::gpd-2 operon::gfp::h2b::cye-1 3'UTR] II; unc-119(ed3) III*, AMJ844: *dpy-2(e8) oxSi487; unc-119(ed3)*, AMJ1020: *dpy-2(jam37) oxSi487; unc-119(ed3); bus-8(jam35) X*) were cultured on plates or in liquid at 15 °C (Stiernagle, 2006).

2.2. Genome editing

Cas9-based genome editing was used to introduce the e2698 mutation (Partridge et al., 2008) into *bus-8* (resulting in BUS-8 [A131V]) in AMJ844 using sgRNA transcribed *in vitro*, a 60-base single-stranded DNA for homology repair, and the correction of *dpy-2(e8)* into *dpy-2(jam37)* as a co-CRISPR marker (Kim et al., 2014; Paix et al., 2014). An edited isolate selected based on failure of AluI (New England Biolabs cat. no: R0137L) restriction digests

was designated as AMJ1020.

2.3. Levamisole sensitivity assay

Batches of three L4-staged worms from AMJ1020, N2, and EG6787 incubated in 10 μ l droplets of varying concentrations of levamisole (tetramisole hydrochloride, Sigma-Aldrich Cat. no.: L9756) in M9 buffer (Stiernagle, 2006) on a coverslip for 60 s were scored as paralyzed if they were unable to perform a half-body bend during the next 60 s.

2.4. Screen of compound library

To generate a sensor for drugs that can disrupt physiological processes including epigenetic regulation in *C. elegans*, we combined two features: (i) transgenerational gene silencing of a fluorescent reporter (*Pmex-5::mCherry::h2b::tbb-2 3'utr::gpd-2 operon::gfp::h2b::cye-1 3' utr*) (Devanapally et al., 2020) and (ii) the *bus-8(e2698)* mutation that is expected to produce a mutant glycosyltransferase protein BUS-8(A131V), resulting in a malformed cuticle (based on (Partridge et al., 2008)). While this strain was generated to facilitate the detection of compounds that disrupt transgenerational epigenetic silencing, the silenced reporters are irrelevant for the effects of the bioactive drugs detected in this study (see Results) and therefore not discussed further.

AMJ1020 was used to screen a compound library (Selleck Chem Cat. no.: L1300 in dimethyl sulfoxide (DMSO)) for compounds that cause increased fluorescence in the red channel (2 s exposure with 4 \times 4 binning using filter cube: 530–560 nm excitation, 570 dichroic, and 590–650 nm emission) and/or in the green channel (varying exposures with 4 \times 4 binning using filter cube: 450–490 nm excitation, 495 dichroic, and 500–550 nm emission). To establish the maximal drug concentration that can be used in the screen, worms were exposed to varying concentrations of the vehicle DMSO and qualitatively assessed for viability. Because we found that a majority of worms could survive for 48 h in a 3% DMSO solution, we used a 3% solution of 10 mM drug dissolved in DMSO to test the effect of each drug on worms. For each compound, 100 μ l of worms from ~12-day liquid culture was aliquoted into each well of 96-well plates along with 3 μ l of 10 mM drug solution and imaged ~48 h later. Worms were imaged after immobilization with levamisole at a fixed magnification on an AZ100 microscope (Nikon) with a Cool SNAP HQ2 camera (Photometrics) after excitation using a C-HGFI Intensilight Hg Illuminator. Drug-exposed and DMSO-exposed AMJ1020 worms were compared with control EG6787 worms imaged (as in (Devanapally et al., 2020)) under the same conditions for each imaging session.

2.5. Secondary assays of positive hits from compound screen

The three drugs identified using the screen were obtained from a second source (Cayman Chemical, cat. no.: 20770 (ticlopidine), 22232 (sertaconazole), 18235 (dexlansoprazole)). Wild-type animals were exposed to newly made solutions of these compounds in DMSO (vehicle) for ~48 h, after which L4-staged worms were selected and exposed for an additional ~24 h before imaging (i.e., young adults were imaged). To examine morphological changes, live worms were mounted on a 3% agarose pad, exposed for ~10 min in 5 μ l of freshly made 3 mM levamisole, and imaged in the red channel without binning (using filter cube: 530–560 nm excitation, 570 dichroic, and 590–650 nm emission) under non-saturating conditions. Differential Interference Contrast (DIC) imaging of the same animals was performed on a Zeiss Axiovert 200 microscope using a 40 \times objective. All images being compared were

identically adjusted using Fiji (NIH) and/or Illustrator (Adobe) for display.

2.6. Statistical analysis

Fractions of animals showing defects were compared using Wilson's estimates with continuity correction (method 4 in (Newcombe, 1998)).

3. Results

To facilitate the identification of bioactive chemicals that interact with *C. elegans*, we generated a drug-sensitive strain where the permeability of the cuticle was enhanced by mutating the predicted glycosyltransferase *bus-8* (Partridge et al., 2008). Consistent with previous reports, we found that mutating *bus-8* made worms more susceptible to the paralytic drug levamisole (Fig. 1a). This strain also had a silenced transgene that could express a green and/or red fluorescent protein if any drug were to disrupt silencing. Therefore, this drug-sensitive strain was grown in liquid culture, exposed to a library of 1443 FDA-approved compounds, and imaged using a fluorescence microscope, to identify any that cause visible changes (Fig. 1b).

Two of the tested compounds - nitazoxanide and curcumin - were expected to cause obvious effects based on prior studies, and did so in our screen. Nitazoxanide caused lethality (as reported in (Somvanshi et al., 2014)), and we additionally detected auto-fluorescent accumulations in Nitazoxanide-exposed worms that were also visible using bright-field microscopy. Curcumin, which fluoresces under our imaging conditions, caused punctate fluorescence within the intestine, likely due to intra-intestinal accumulation (Kunwar et al., 2008; Shen et al., 2019). While none of the compounds revived the silenced transgene, three compounds that do not fluoresce as solutions under our imaging conditions caused increased fluorescence in the pharyngeal region: ticlopidine, sertaconazole, and dexamproprazole. Similar increases were observed in wild-type animals without the silenced transgene and malformed cuticle (Fig. 2), demonstrating that the standard laboratory strain is susceptible to the effects of these drugs.

Each drug caused a distinct change in the pharyngeal region that was evident even under low magnification using bright-field microscopy. Closer examination of worms exposed to ticlopidine or sertaconazole revealed blebs in the procorpus and metacorpus regions of the pharynx with associated lethality (Fig. 2a-c): ticlopidine caused large blebs and 28% lethality (22/78 dead vs 1/39 in

DMSO) and sertaconazole caused small blebs and 67% lethality (39/58 dead vs 1/39 in DMSO). These characteristic blebs also occurred upon acute exposure of fourth larval (L4) staged animals to either compound for 48 h (Fig. 2a-c, 45% of ticlopidine-exposed live animals and 79% of sertaconazole-exposed live animals). Both kinds of changes with associated lethality are reminiscent of the recent demonstration of chemical accumulation in the marginal cells of the pharynx that can concentrate sterols and other hydrophobic compounds (Kamal et al., 2019). While ticlopidine and sertaconazole were not identified in this study (Peter J. Roy, personal communication), a wide array of other compounds similarly caused two kinds of changes in the pharynx. One class of chemicals, with smaller topological polar surface areas on average, caused accumulation of spheres that appear similar to the large blebs induced by ticlopidine (e.g., wact-209). The other class, with larger topological polar surface areas on average, caused accumulation of crystals that appear similar to the small blebs induced by sertaconazole (e.g., wact-43). Consistently, the topological polar surface area of ticlopidine (31.5 \AA^2) is smaller than that of sertaconazole (55.3 \AA^2). However, the molecular basis of the distinct morphologies and the mechanism(s) that underlie lethality require further study.

Dexamproprazole, on the other hand, caused a darkening of the pharynx that was visible under low magnification in L4-staged or young adult animals (11/82 animals). Closer examination of these animals (Fig. 2d) revealed an obstruction in the lumen of the pharynx (6/11 animals) and/or a molting defect (8/11 animals). Unlike the changes caused by ticlopidine or sertaconazole, the changes caused by dexamproprazole were not associated with lethality (0/38 dead upon acute exposure at the L4 stage) or apparent bleb formation and required exposure during larval development.

Thus, three FDA-approved drugs cause lethality and/or easily detected morphological changes in *C. elegans* that could be analyzed to understand their mechanisms of cellular uptake, modes of action, and spectrum of side effects.

4. Discussion

About 4.4 million people in the United States are estimated to have been prescribed ticlopidine, sertaconazole, or dexamproprazole in a 7-year period (estimate based on those insured between 2007 and 2014 (Quinn and Shah, 2017)). Ticlopidine is thought to inhibit platelet aggregation by blocking an adenosine-diphosphate receptor (McTavish et al., 1990) and is sometimes used during the placement of stents in coronary arteries. Sertaconazole is thought to inhibit fungal growth by disrupting fungal cell membranes (Carrillo-Muñoz et al., 2005) and is used to treat athlete's foot. Dexamproprazole is thought to inhibit gastric acidity by blocking a proton pump (Fock and Ang, 2008) and is used to treat gastroesophageal reflux and peptic ulcers. Intriguingly, the set of genes affected by ticlopidine in human cell lines are negatively connected with genes affected by lansoprazole, a racemic mixture of levansoprazole and dexamproprazole (2nd rank on CMap (Subramanian et al., 2017)), suggesting a possible convergence of these two disparate compounds on the same molecular effectors.

Accumulation of drugs in the marginal cells of the *C. elegans* pharynx requires sphingomyelin because both spherical accumulations - like those of ticlopidine (Fig. 2b) - and crystalline accumulations - like those of sertaconazole (Fig. 2c) - do not occur in animals lacking the sphingomyelin synthase SMS-5 (Kamal et al., 2019). However, the lethality persisted despite absence of accumulations in *sms-5(-)* animals for 100% of sphere-forming compounds and for 53% of crystal-forming compounds (Kamal et al.,

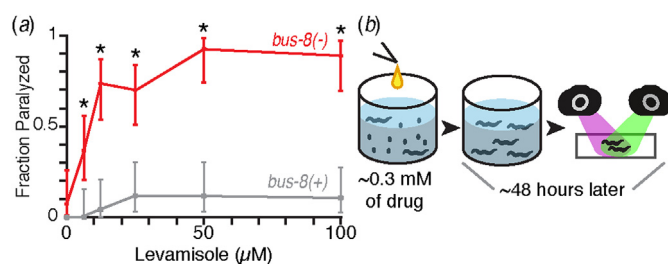


Fig. 1. Development and use of a strain for the sensitive detection of bioactive compounds. (a) Loss of *bus-8* function makes *C. elegans* hypersensitive to the paralytic drug levamisole, consistent with increased permeability to small molecules. Fractions of animals with a mutation in *bus-8* (*bus-8(-)*) and animals without the mutation (*bus-8(+)*) that were paralyzed by different concentrations of levamisole are shown. Error bars indicate 95% CI and asterisks indicate $p < 0.05$, Wilson's estimates. (b) Schematic of screen for drug-induced changes using a sensor strain with silenced *gfp* and *mCherry* reporters. Liquid cultures of the sensor strain were exposed to ~0.3 mM of each drug from a library of 1443 FDA-approved compounds for 48 h and imaged using a fluorescence microscope in red and green channels.

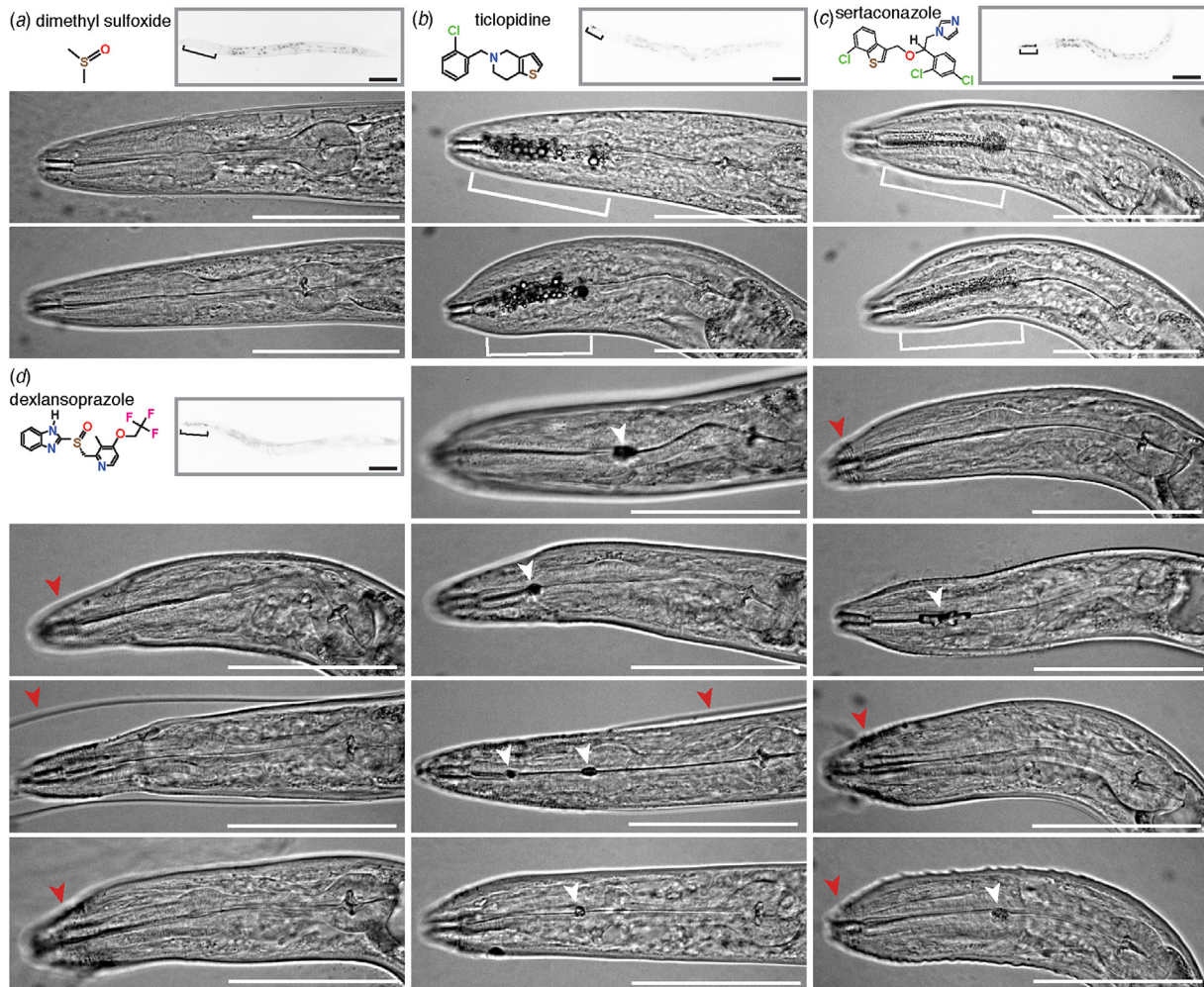


Fig. 2. Three FDA-approved drugs can alter the morphology of *C. elegans*. (a-c) Ticlopidine and sertaconazole cause distinct changes in the pharynx upon acute exposure. Unlike the vehicle dimethyl sulfoxide (a), ticlopidine (b) and sertaconazole (c) alter the pharyngeal region in wild-type animals. For each compound, chemical structures (top left), induced changes in fluorescence (brackets) at lower magnification in the red channel (top right; scale bar = 100 μm) and induced changes in morphology of the pharynx (brackets), if any, at higher magnification (middle and bottom; scale bar = 50 μm) are shown. Changes in pharyngeal morphology were observed in 0/38 animals upon DMSO exposure, in 25/56 animals upon ticlopidine exposure ($p < 0.05$, Wilson's estimates) and in 15/19 animals upon sertaconazole exposure ($p < 0.05$, Wilson's estimates). Two different animals are shown for each compound to illustrate the reproducibility of the distinct changes observed in ticlopidine (b) and in sertaconazole (c). (d) Dexlansoprazole causes defects in molting and/or a blockage within the pharyngeal lumen upon exposure during larval development. Top left, The chemical structure and induced changes in fluorescence (brackets) at lower magnification in the red channel (scale bar = 100 μm) are shown. Other panels, The defects caused by dexlansoprazole varied from worm to worm. A change in the pharyngeal region could be discerned under low magnification in 11/82 animals and the 11 animals that exhibit a molting defect (red arrowhead) and/or blockage of the pharyngeal lumen (white arrowhead) are shown.

2019). Furthermore, while *sms-5(-)* worms became resistant to some crystal forming compounds, they became hypersensitive to others (Kamal et al., 2019). These considerations suggest preliminary hypotheses for how ticlopidine and sertaconazole could depend on the sphingomyelin content of plasma membranes. Ticlopidine likely requires sphingomyelin generated by SMS-5 in the marginal cells of *C. elegans* for visible accumulations, but causes lethality independent of these accumulations. Sertaconazole could either require SMS-5 for both accumulations and lethality or cause lethality at lower concentrations in *sms-5(-)* animals. Thus, the mechanism(s) that ticlopidine and sertaconazole rely on to cause lethality in *C. elegans* could be independent. Nevertheless, sphingomyelin content of plasma membranes could be a conserved feature that dictates the interaction of these two drugs with human tissues. The sphingomyelin content of most mammalian tissues ranges from 2% to 15% of the total phospholipids (Koval and Pagano, 1991). The higher levels found in some tissues (e.g., erythrocytes, ocular lenses and the brain) could make them differentially

susceptible to the effects of these drugs. Finally, because sphingomyelin-rich regions form plasma membrane rafts that concentrate receptors (Chakraborty and Jiang, 2013), these drugs could also disrupt cellular signaling.

Dexlansoprazole could disrupt a wide range of processes to cause the observed molting defects (Fig. 2d). More than 150 genes can be disrupted to interfere with the release of the old cuticle and/or production of a new cuticle to cause molting defects in *C. elegans* (Frand et al., 2005). Many of these genes encode conserved molecules involved in vesicular trafficking, steroid-hormone signaling, developmental timing, and hedgehog-like signaling (reviewed in (Lažetić and Fay, 2017)). The molting defects observed thus far have been classified into five broad categories based on the location of the leftover old cuticle: complete encasement, partial release in the head region, corset along the central body, constriction in the middle, and surface attachment. The defects seen upon exposure to dexlansoprazole do not appear to fall neatly within any one of these broad categories (see variety in Fig. 2d) and in addition includes the

blockage observed within the pharyngeal lumen (white arrowheads, Fig. 2d). Thus, identifying the molecular target(s) of dexlansoprazole in *C. elegans* has the potential to inform both the biology of molting and conserved processes that could be similarly disrupted in humans.

Further analyses using each drug and its variants are necessary to identify active metabolites (if any) and to determine drug-induced molecular changes in *C. elegans* that lead to the observed morphological changes and/or lethality. We speculate that similar exploration of approved drugs using a variety of model organisms could open avenues of research that reveal unanticipated effects of accepted medicines.

Author statement

Kyle Galford: Methodology, Formal analysis, Investigation, Writing - original draft, Visualization, **Antony Jose:** Conceptualization, Methodology, Formal analysis, Resources, Visualization, Writing - review & editing, Supervision, Project administration, Funding acquisition.

Declaration of competing interest

The authors declare that they have no known competing financial interests or personal relationships that could have appeared to influence the work reported in this paper.

Acknowledgements

We thank Edwin Zhang for contributions towards assay development; Pravurutha Raman for help with introducing the *bus-8* mutation; and Norma Andrews, Tom Kocher and members of the Jose lab for comments on the manuscript. This work was supported by the Tier 1 Faculty Incentive Program at the University of Maryland and in part by a grant from the NIH [R01 GM124356].

References

- Carrillo-Muñoz, A.J., Giusiano, G., Ezkurra, P.A., Quindós, G., 2005. Sertaconazole: updated review of a topical antifungal agent. *Expert Rev. Anti Infect. Ther.* 3, 333–342.
- Chakraborty, M., Jiang, X.C., 2013. Sphingomyelin and its role in cellular signaling. *Adv. Exp. Med. Biol.* 991, 1–14.
- Devanapally, S., Raman, P., Allgood, S., Etefa, F., Diop, M., Chey, M., Lin, Y., Cho, Y.E., Yin, R., Jose, A.M., 2020. Recovery from transgenerational RNA silencing is driven by gene-specific homeostasis. [10.1101/148700v3](https://doi.org/10.1101/148700v3).
- Donovan, K.A., An, J., Nowak, R.P., Yuan, J.C., Fink, E.C., Berry, B.C., Ebert, B.L., Fischer, E.S., 2018. Thalidomide promotes degradation of SALL4, a transcription factor implicated in Duane Radial Ray syndrome. *eLife* 7, e38430.
- Ferreira, D.W., Chen, Y., Allard, P., 2014. Using the alternative model *C. elegans* in reproductive and developmental toxicology studies. In: Faqi, A. (Ed.), *Developmental and Reproductive Toxicology*. Humana Press, New York, NY, pp. 261–278. *Methods in Pharmacology and Toxicology*.
- Fock, K.M., Ang, T.L., 2008. Dexlansoprazole, a modified release formulation of an enantiomer of lansoprazole, for the treatment of reflux esophagitis. *Curr. Opin. Invest. Drugs* 9, 1108–1115.
- Frand, A.R., Russel, S., Ruvkun, G., 2005. Functional genomic analysis of *C. elegans* molting. *PLoS Biol.* 3, e132.

- Fratta, I.D., Sigg, E.B., Maiorana, K., 1965. Teratogenic effects of thalidomide in rabbits, rats, hamsters, and mice. *Toxicol. Appl. Pharmacol.* 7, 268–286.
- Hunt, P.R., 2017. The *C. elegans* model in toxicity testing. *J. Appl. Toxicol.* 37, 50–59.
- Kaletta, T., Hengartner, M.O., 2006. Finding function in novel targets: *C. elegans* as a model organism. *Nat. Rev. Drug Discov.* 5, 387–399.
- Kamal, M., Moshiri, H., Magomedova, L., Han, D., Nguyen, K.C.Q., Yeo, M., Knox, J., Bagg, R., Won, A.M., Szlapa, K., Yip, C.M., Cummins, C.L., Hall, D.H., Roy, P.J., 2019. The marginal cells of the *Caenorhabditis elegans* pharynx scavenge cholesterol and other hydrophobic small molecules. *Nat. Commun.* 10, 3938.
- Kim, H., Ishidate, T., Ghanta, K.S., Seth, M., Conte, D., Shirayama, M., Mello, C.C., 2014. A co-CRISPR strategy for efficient genome editing in *Caenorhabditis elegans*. *Genetics* 197, 1069–1080.
- Kim, W., Underwood, R.S., Greenwood, I., Shaye, D.D., 2018. OrthoList 2: a new comparative genomic analysis of human and *Caenorhabditis elegans* genes. *Genetics* 210, 445–461.
- Koval, M., Pagano, R.E., 1991. Intracellular transport and metabolism of sphingomyelin. *Biochim. Biophys. Acta* 1082, 113–125.
- Krumholz, H.M., Ross, J.S., Presler, A.H., Egilman, D.S., 2007. What have we learnt from Vioxx? *BMJ* 334, 120–123.
- Kunwar, A., Barik, A., Mishra, B., Rathinasamy, K., Pandey, R., Priyadarsini, K.I., 2008. Quantitative cellular uptake, localization and cytotoxicity of curcumin in normal and tumor cells. *BBA-Gen Subjects*. 1780, 673–679.
- Lažetić, V., Fay, D.S., 2017. Molting in *C. elegans*. *Worm* 6, e1330246.
- Lenz, W., Pfeiffer, R.A., Kosenow, W., Hayman, D.J., 1962. Thalidomide and congenital abnormalities. *Lancet* 279, 45–46.
- Matyskiela, M.E., Couto, S., Zheng, X., Lu, G., Hui, J., Stamp, K., Drew, C., Ren, Y., Wang, M., Carpenter, A., Lee, C.W., Clayton, T., Fang, W., Lu, C.C., Riley, M., Abdubek, P., Blease, K., Hartke, J., Kumar, G., Vessey, R., Rolfe, M., Hamann, L.G., Chamberlain, P.P., 2018. SALL4 mediates teratogenicity as a thalidomide-dependent cereblon substrate. *Nat. Chem. Biol.* 14, 981.
- McBride, W., 1961. Thalidomide and congenital malformations. *Lancet* 278, 1358.
- McTavish, D., Faulds, D., Goa, K.L., 1990. Ticlopidine. An updated review of its pharmacology and therapeutic use in platelet-dependent disorders. *Drugs* 40, 238–259.
- MedWatch, 2020. The FDA Safety Information and Adverse Event Reporting Program. U.S. Food and Drug Administration, Rockville, Md. <http://purl.access.gpo.gov/GPO/LPS81698>. (Accessed 7 December 2020).
- Mullard, A., 2019. 2018 FDA drug approvals. *Nat. Rev. Drug Discov.* 18, 85–89.
- Newcombe, R., 1998. Two-sided confidence intervals for the single proportion: comparison of seven methods. *Stat. Med.* 17, 857–872.
- Overington, J.P., Al-Lazikani, B., Hopkins, A.L., 2006. How many drug targets are there? *Nat. Rev. Drug Discov.* 5, 993–996.
- Paix, A., Wang, Y., Smith, H.E., Lee, C.Y., Calidas, D., Lu, T., Smith, J., Schmidt, H., Krause, M.W., Seydoux, G., 2014. Scalable and versatile genome editing using linear DNAs with microhomology to Cas9 Sites in *Caenorhabditis elegans*. *Genetics* 198, 1347–1356.
- Partridge, F.A., Tearle, A.W., Gravato-Nobre, M.J., Schafer, W.R., Hodgkin, J., 2008. The *C. elegans* glycosyltransferase BUS-8 has two distinct and essential roles in epidermal morphogenesis. *Dev. Biol.* 317, 549–559.
- Quinn, J., Shah, N.H., 2017. A dataset quantifying polypharmacy in the United States. *Sci. Data* 4, 170167.
- Shen, P., Zhang, R., McClements, D.J., Park, Y., 2019. Nanoemulsion-based delivery systems for testing nutraceutical efficacy using *Caenorhabditis elegans*: demonstration of curcumin bioaccumulation and body-fat reduction. *Food Res. Int.* 120, 157–166.
- Somvanshi, V.S., Ellis, B.L., Hu, Y., Aroian, R.V., 2014. Nitazoxanide: nematocidal mode of action and drug combination studies. *Mol. Biochem. Parasitol.* 193, 1–8.
- Stiernagle, T., 2006. Maintenance of *C. elegans*. *WormBook*. The *C. elegans* Research Community.
- Subramanian, A., Narayan, R., Corsello, S.M., Peck, D.D., Natoli, T.E., Lu, X., Gould, J., Davis, J.F., Tubelli, A.A., Asiedu, J.K., Lahr, D.L., Hirschman, J.E., Liu, Z., Donahue, M., Julian, B., Khan, M., Wadden, D., Smith, I.C., Lam, D., Liberzon, A., Toder, C., Bagul, M., Orzechowski, M., Enache, O.M., Piccioni, F., Johnson, S.A., Lyons, N.J., Berger, A.H., Shamji, A.F., Brooks, A.N., Vrcic, A., Flynn, C., Rosains, J., Takeda, D.Y., Hu, R., Davison, D., Lamb, J., Ardlie, K., Hogstrom, L., Greenside, P., Gray, N.S., Clemons, P.A., Silver, S., Wu, X., Zhao, W.N., Read-Button, W., Wu, X., Haggarty, S.J., Ronco, L.V., Boehm, J.S., Schreiber, S.L., Doench, J.G., Bittker, J.A., Root, D.E., Wong, B., Golub, T.R., 2017. A next generation connectivity map: 1,100 platform and the first 1,000,000 profiles. *Cell* 171, 1437–1452.